Struct Multidisc Optim
DOI 10.1007/s00158-017-1747-8

INDUSTRIAL APPLICATION

Reliability-based and deterministic design optimization of a FSAE brake pedal: a risk allocation analysis

José Romero[1] · **Nestor Queipo**[2]

Received: 16 January 2017 / Revised: 12 May 2017 / Accepted: 19 June 2017

Abstract While probabilistic designs can translate into significant weight savings through better risk allocation, deterministic design optimization remains widely used in industry. To promote the use of probabilistic designs among engineering students and practitioners, this work solves reliability based design optimization (RBDO) and deterministic design optimization (DDO) models of a FSAE brake pedal with multiple failure modes (stress and buckling) with their relative performance evaluated through a risk allocation analysis. The problems of interest were systematically solved through the following steps: i) topology optimization to specify the brake-pedal shape, ii) numerical 3D brake-pedal modeling under uncertainty for stress and buckling analysis, iii) mass (M), maximum von Mises stress (S_{max}) and buckling load factor (f_{buck}) surrogate modeling, iv) global sensitivity analysis and surrogate model selection, and v) surrogate-based RBDO and DDO with risk allocation analysis. Results show that when compared to DDO with alternative safety factors, for the same probability of system failure, the RBDO brake pedal designs were significantly lighter and more robust (less mass variability).

Keywords Brake pedal · Formula SAE · Probabilistic optimization · Risk allocation

✉ Nestor Queipo
nqueipo@ica.luz.edu.ve

José Romero
jlromero@ica.luz.edu.ve

[1] Department of Mechanical Engineering, University of Zulia, Maracaibo, Venezuela

[2] Applied Computing Institute, University of Zulia, Maracaibo, Venezuela

Nomenclature

Symbol	Explanation
c_i	Design parameters
Cov(.)	Covariance function
CT	Computational time
d	Vector of random design variables
d_i	Random design variables
E	Young's modulus
$E_{0.05}$	Characteristic value of Young's modulus
f(.)	Function of interest (M, S_{max} or f_{buck}) in global sensitivity analysis
f(**x**)	Regression function of x in Kriging model
f_{buck}(.)	Buckling load factor function
f_0	Mean value of function of interest vector f(ξ)
g_i(.)	DDO constraint functions
G_j(.)	Limit state function for failure mode j
G_1(.)	Limit state function of stress condition
G_2(.)	Limit state function of buckling condition
I	Counter or indicator function
p	Vector of random design parameters
$\mathbf{p}^*$	Vector of mean values of random geometric design parameters and characteristic value of Young's modulus ($E_{0.05}$)
M(.)	Brake pedal mass function
$\mathbf{M}(.)$	Random brake pedal mass function
n	Number of sample points
n_{rv}	Number of random variables
P(F)	Probability of system failure
P(.)	Probability of the statement within the braces to be true

P_{fT}	Target probability of system failure
$\mathbf{R}(.)$	Correlation function
SF	Preestablished safety factor values
S_i, S_{ij} and S_{ijk}	Main, second order, and third order sensitivity index, respectively
S_{itotal}	Total sensitivity index of random variable i
S_y	Material yield strength
$S_{y0.05}$	Characteristic value of material yield strength
$S_{max}(.)$	Maximum von Mises stress function
tol_i	Manufacturing tolerance probability distribution of $\mathbf{d_i}$
t_f	Computational time of one ten-fold cross-validation run
V	Total variance of random variables
V_i, V_{ij} and V_{ijk}	Partial variance of, random variable i, interaction effects of random variables ij and ijk, respectively
V_{zi}	Sum of partial variances of all possible subsets variables in $\mathbf{Z}_i$.
$\mathbf{x}$	Vector of random variables, $\mathbf{x} = [\mathbf{d}, \mathbf{p}]$ or input variables vector
$\mathbf{x_i}$	Random variables or vector of the input variable at the ith sample point
y	Vector of output variables
$\hat{y}(\mathbf{x})$	Surrogate prediction function
$Z(\mathbf{x})$	Aleatory function with mean zero, and nonzero covariance
$\mathbf{Z}_i$	Vector containing $x_1, x_2, x_3, \ldots, x_n$ $(n \neq i)$ random variables
β_0, β_i, β_{ii},β_{ij}	Polynomial regression coefficients
γ	Safety factor index
ε	Surrogate model error
ε_b	Buckling load factor surrogate model error
ε_M	Mass surrogate model error
ε_S	Maximum von Mises stress surrogate model error
λ_i	Coefficient of the basis function
$\boldsymbol{\mu_d}$	Vector of mean values of random design variables
μ_M	Mass mean value
$\boldsymbol{\mu_p}$	Vector of mean values of random design parameters
μ_{Error}	Mean value of surrogate relative error
ν	Poisson's ratio
ξ and ξ'	Two independent matrices with columns representing brake pedal random variables uniformly distributed in the range of $[\mathbf{x}^L\ \mathbf{x}^U]$
$\xi'^{\mathbf{i}}$, $\xi'^{\mathbf{ij}}$, $\xi'^{\mathbf{ijk}}$	Matrices ξ' in which the columns of random variables i, i and j, and i, j and k are replaced by the corresponding elements in matrix ξ, respectively
ρ	Material density
σ^2	Process variance in Kriging model
σ_{Error}	Standard deviation value of surrogate relative error
σ_M	Mass standard deviation value

1 Introduction

Risk allocation (e.g., Suzuki and Haftka 2014) in structural design under uncertainty (aleatory and epistemic) highlights a well-known fact: deterministic approaches may lead to extremely conservative or unknowingly dangerous designs; see, for example, Qu et al. (2003), Papadrakakis et al. (2005), Plšek et al. (2007), Beck and de Santana Gomes (2012), Gu et al. (2013). However, DDO-deterministic design optimization remains widely used in vital industries such as the aerospace and automotive, e.g., Mårtensson et al. (2015), Gern (2015), Allison et al. (2015), Lyu and Martins (2015), Liu et al. (2015), Deb et al. (2015). A key element of a long term solution to alleviate this shortcoming among practitioners may be: early participation of engineering students in meaningful and benchmarked probabilistic design efforts widely available.

For a given safety factor and failure modes, a risk allocation analysis establishes the corresponding probability of system failure, conducts a RBDO-reliability-based design optimization (Frangopol 1985; Lee 1987), and computes the risks associated with each failure mode. Probabilistic designs often show significant gains (weight reduction) for a given probability of failure with deterministic designs offering excessive protection with respect to alternative failure modes. In particular, using RBDO weight reductions were obtained by Acar and Haftka (2007) with analytical models for aircraft wing and tail structures, allocating slightly more risk to the wings while reducing it for the tail; Villanueva et al. (2009) with a 3D structural model of an integrated thermal protection system (ITPS) and a 1-D thermal analysis, allocating more risk to thermal and stress failure while reducing it to buckling failure; Venter and Scotti (2012) with an analytical model of a stepped cantilevered beam with three segments, allocating risk roughly equal to the weight ratio of the segments; and Suzuki and Haftka (2014) with an analytical model two-bar truss subject to random horizontal loads, i.e., summer and winter storm wind force, allocating slightly more risk to the summer load and reducing it for winter load. Note that most applications have been limited to analytical models and all have been domain-specific and may not have widespread appeal among students and practitioners.

On the other hand, structural design plays a significant role in multidisciplinary engineering projects promoted by professional societies such as ASME-American Society of Mechanical Engineers and SAE-Society of Automotive Engineers (ASME 2016; SAE international 2016a) at universities. Such projects help the development of the next generation engineering workforce by taking students out of the classroom and allowing them to apply textbook theories to real work experiences. For example, the Formula SAE project (SAE international 2016b, c) with the annual participation of 2470 students from 120 university teams, promotes careers and excellence in engineering in the automotive industry including research, design, manufacturing, testing, developing, marketing, management and finances. In particular, each component in a single seater FSAE vehicle must be safe and lightweight in order to decrease the vehicle mass, and take the most advantage of the engine power.

Before the year 2011, FSAE teams often reduced the safety factor in conventional design methods for mass reduction and underestimated the loads applied to the pedal board component, leading to brake pedal failure during dynamic competitions and a new regulation (SAE international 2011) on the minimum design load, i.e., 2000 N. The results of considering the new regulation and the use of safety factor-based conventional design methods: potentially oversized or risk-prone brake pedals. The brake pedal design under uncertainty of FSAE vehicles represents: i) an easy to understand structural problem among engineering students and practitioners around the world yet relevant to aerospace and automotive industrial environments, and ii) an opportunity to illustrate the weight savings potential of RBDO with respect to DDO by balancing the risks among failure modes (stress and buckling).

This work formulates and solves RBDO and DDO models with multiple failure modes (stress and buckling) of a FSAE brake pedal with their relative performance evaluated through a risk allocation analysis. The problems of interest were systematically solved through the following steps: i) topology optimization to specify the brake-pedal shape, ii) numerical 3D brake-pedal modeling under uncertainty for stress and buckling analysis, iii) mass (M), maximum von Mises stress (S_{max}) and buckling load factor (f_{buck}) surrogate modeling, iv) global sensitivity analysis and surrogate models selection, and v) surrogate-based RBDO and DDO with risk allocation analysis.

The rest of the paper is structured as follows: Section 2 RBDO and DDO problem formulation, Section 3 brake pedal numerical model under uncertainty, Section 4 mass and failure modes surrogate modeling, Section 5 global sensitivity analysis and surrogate models selection, Section 6 surrogate-based RBDO and DDO with risk allocation analysis, Section 7 results and discussion, and Section 8 conclusions.

2 RBDO and DDO problem formulation

Given a FSAE brake pedal model with a set of design variables (e.g., Fig. 1) and geometric parameters (e.g., Fig. 2), the problems of interest can be formulated as follows:

RBDO	DDO
Find $\mathbf{d} = [d_1, d_2, \dots, d_n]$ that	Find $\boldsymbol{\mu}_\mathbf{d} = [\mu_{d_1}, \mu_{d_2}, \dots, \mu_{d_n}]$ that
$\text{Min} \quad M(\boldsymbol{\mu}_\mathbf{d}, \boldsymbol{\mu}_\mathbf{p})$ (1)	
subject to:	subject to:
$P(\mathbf{F}) = P[G_1(\mathbf{x}) \le 0 \cup G_2(\mathbf{x}) \le 0] \le P_{fT}$ (2)	$\frac{S_{y_{0.05}}}{\gamma} - S_{max}(\boldsymbol{\mu}_\mathbf{d}, \boldsymbol{\mu}_\mathbf{p}) \ge 0$ (3)
	$f_{buck}(\boldsymbol{\mu}_\mathbf{d}, \mathbf{p}^*) - \gamma \ge 0$ (4)
$d_i{}^L \le d_i \le d_i{}^U; \quad i = 1,2, \dots, n$	$\mu_{d_i}{}^L \le \mu_{d_i} \le \mu_{d_i}{}^U; \quad i = 1,2, \dots, n$

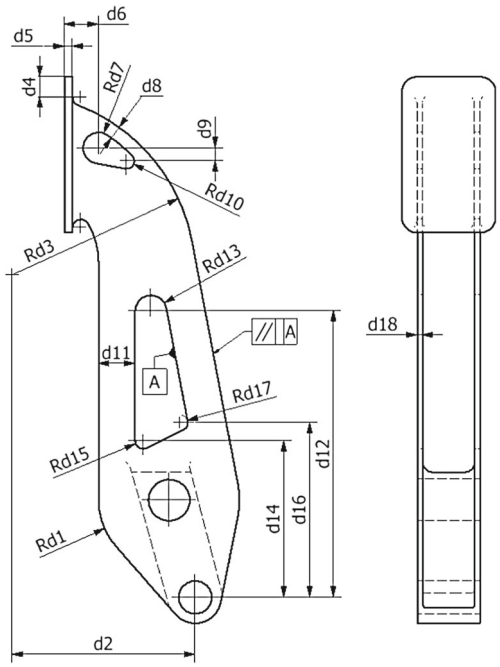

Fig. 1 FSAE brake pedal geometrical model with design variables

where superscripts L and U denote lower and upper bounds, respectively, and:

$$G_1(\mathbf{x}) = S_y - S_{max}(\mathbf{x})(1 + \varepsilon_S) \quad (5)$$

$$G_2(\mathbf{x}) = f_{buck}(\mathbf{x})(1 + \varepsilon_b) - 1 \quad (6)$$

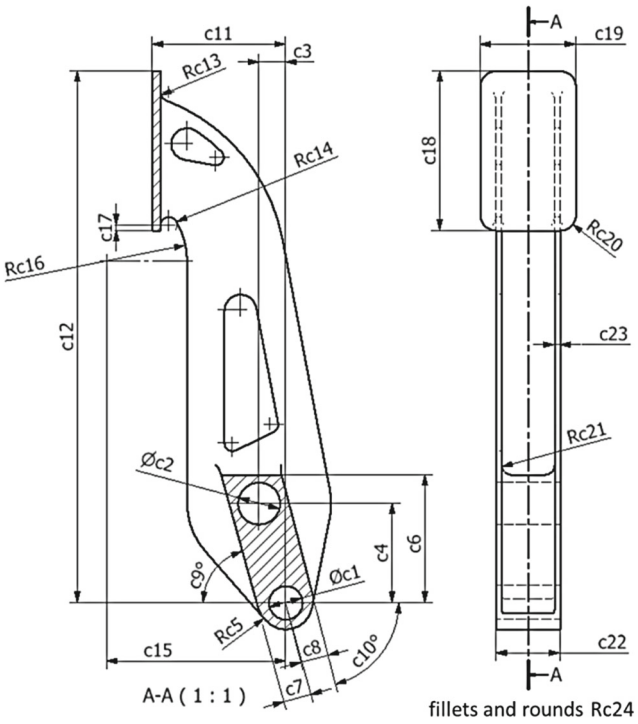

Fig. 2 FSAE brake pedal geometrical model with design parameters

3 Brake pedal numerical model under uncertainty

3.1 Brake pedal geometrical model

The parametrization of the brake pedal geometrical model includes a set of 18 design variables (Fig. 1 and Table 1) and 24 parameters (Fig. 2 and Table 2). The design variable bounds (Table 1) allow a significant number of alternative shapes. The geometrical configuration of interest was the result of topology optimization (Bendsoe and Kikuchi 1988; Rozvany et al. 1992; Mlejnek 1992) followed by a smoothing and validation mesh, while avoiding regions of high stress concentrations (Fig. 3). The 3D topology optimization was conducted with the assistance of a MATLAB program reported by Liu and Tovar (2014).

3.2 Uncertainty model

To account for modeling and computational limitations, normally distributed error terms are included in the mass (ε_M), maximum von Mises stress (ε_S) and buckling load factor (ε_S) surrogate models (Lian and Kim 2006; Acar and Solanki 2009; Neufeld et al. 2010; Ravishankar et al. 2011; Rangavajhala et al. 2012). On the other hand, the manufacturing tolerances (Tables 1 and 2) are modeled by uniform distributions following the principle of maximum entropy (Acar et al. 2010). These tolerances were defined using the ISO 2768–1 standard (ISO 1989) with tolerance class designations coarse and medium for linear and broken edges, and angular dimensions, respectively.

The material used in the brake pedal design was Aluminum 6063-T5 with probability distributions for selected mechanical properties identified (Fig. 4) by Barroso (2015) from experimental data sets (ASTM 2007) and their suitableness confirmed using the Anderson-Darling goodness-of-fit test (D'Agostino 1986). Table 3 shows the material property probability distributions used in this work.

3.3 Assumptions, load and boundary conditions

The assumptions are: material is homogeneous and isotropic, maximum load uniformly distributed and gradually applied (no impact), finite element (FE) stress analysis was static and linear, and FE buckling analysis was nonlinear with enabled large deflections.

The brake pedal shall withstand a force of 2000 N without any failure of the brake system or pedal box (SAE International 2016d), with pin and planar boundary conditions as shown in Fig. 5. Note that the domain of the brake pedal numerical model must be complete (Fig. 5) to perform a correct buckling analysis, that is, a reduction of the computational time by the application of the symmetry principle is not an option.

Table 1 FSAE brake pedal design variable bounds and tolerances

Design variable	Bounds (mm)		Manufacturing tolerance (mm)	Design variable	Bounds (mm)		Manufacturing tolerance (mm)
	lower	upper			lower	upper	
d1	27	33	U(-0.8,0.8)	d10	2	6	U(-0.3,0.3)
d2	70	80	U(-0.8,0.8)	d11	8	18	U(-0.5,0.5)
d3	70	87	U(-0.8,0.8)	d12	80	115	U(-0.8,0.8)
d4	2	8	U(-0.5,0.5)	d13	2	8	U(-0.5,0.5)
d5	2	4	U(-0.3,0.3)	d14	60	74	U(-0.8,0.8)
d6	10	18	U(-0.5,0.5)	d15	2	4	U(-0.3,0.3)
d7	2	8	U(-0.5,0.5)	d16	60	74	U(-0.8,0.8)
d8	5	10	U(-0.5,0.5)	d17	2	4	U(-0.3,0.3)
d9	4	22	U(-0.5,0.5)	d18	2	6	U(-0.3,0.3)

3.4 Mesh control study

Table 4 shows the results of the mesh control study of nine (9) maximum lengths of finite elements for the brake pedal numerical model presented in Table 5. Note that the default mesh generated by the structural analysis tool (ANSYS Workbench) offered the highest maximum von Mises stress (S_{max}) and buckling factor (f_{buck}) calculation errors compared with best results (lowest S_{max} and f_{buck} calculation errors) obtained using a 1 mm maximum finite element length.

Figure 6 depicts the adopted mesh representing a compromise solution between S_{max} and f_{buck} calculation errors and computational time with a 3 mm maximum finite element length. The computational times with the selected mesh are approximately 6 and 7 s per structural and buckling analysis, respectively, on an Intel Core i7-3630QM CPU @ 2.40 Hz computer with 6 GB of RAM memory.

4 Mass, maximum von Mises stress and buckling load factor surrogate modeling

The basic steps in surrogate modelling (Queipo et al. 2005; Wang and Shan 2007; Forrester and Keane 2009; Han and Zhang 2012) are: i) design of experiments (DOE), ii) numerical simulations at DOE, and iii) construction of surrogate models from DOE (input) and numerical simulation results (output). Figure 7 illustrates the surrogate modeling process for a function with two (2) input variables (x_1, x_2) and one (1) output variable (y) constructed from a design of experiment of sixteen (16) samples and the corresponding numerical simulations.

The functions of interest in this work (M, S_{max} and f_{buck}) originally exhibit forty three (43) random variables among design (18), geometric parameters (24) and the Young's modulus, namely polynomial regression, Kriging, and radial basis

Table 2 FSAE brake pedal design parameter mean values and tolerances

Design parameters	Mean value	Manufacturing tolerance	Design parameters	Mean value	Manufacturing tolerance
c1	12.7 mm	U(0.000,0.018)* mm	c13	3.175 mm	U(-0.3,0.3) mm
c2	15.875 mm	U(0.000,0.018)* mm	c14	3.175 mm	U(-0.3,0.3) mm
c3	10 mm	U(-0.5,0.5) mm	c15	67 mm	U(-0.8,0.8) mm
c4	37.32 mm	U(-0.8,0.8) mm	c16	30 mm	U(-0.5,0.5) mm
c5	10 mm	U(-0.5,0.5) mm	c17	2 mm	U(-0.2,0.2) mm
c6	48 mm	U(-0.8,0.8) mm	c18	60 mm	U(-0.8,0.8) mm
c7	10 mm	U(-0.5,0.5) mm	c19	36 mm	U(-0.8,0.8) mm
c8	10 mm	U(-0.5,0.5) mm	c20	6 mm	U(-0.3,0.3) mm
c9	75°	U(-0.5,0.5) °	c21	4 mm	U(-0.3,0.3) mm
c10	75°	U(-0.5,0.5) °	c22	24 mm	U(-0.5,0.5) mm
c11	50 mm	U(-0.8,0.8) mm	c23**	d18	U(-0.3,0.3) mm
c12	200 mm	U(-1.2,1.2) mm	c24	2 mm	U(-0.2,0.2) mm

*ISO clearance fit, H7/f6

**relation parameter

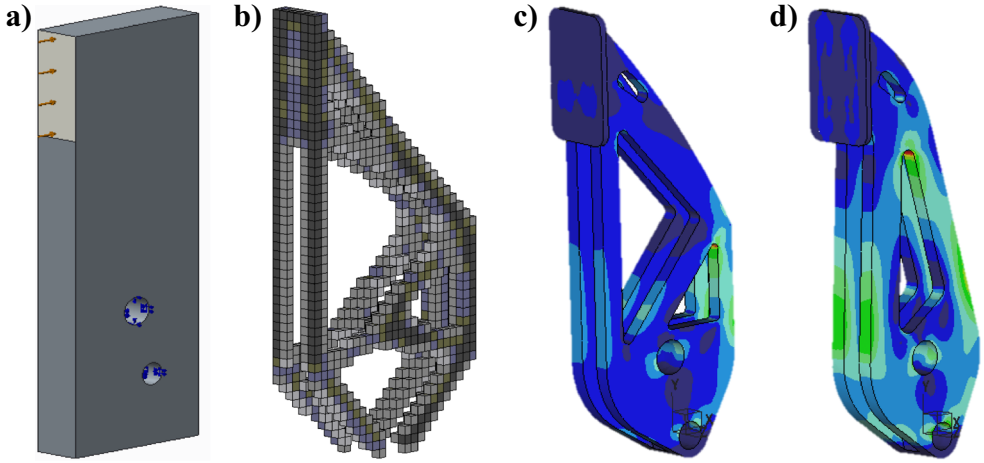

Fig. 3 Different stages leading to the geometrical configuration of interest, (**a**) initial design domain, (**b**) topology optimized brake pedal, (**c**) smoothing and validation mesh, and (**d**) configuration of interest (while avoiding regions of high stress concentrations)

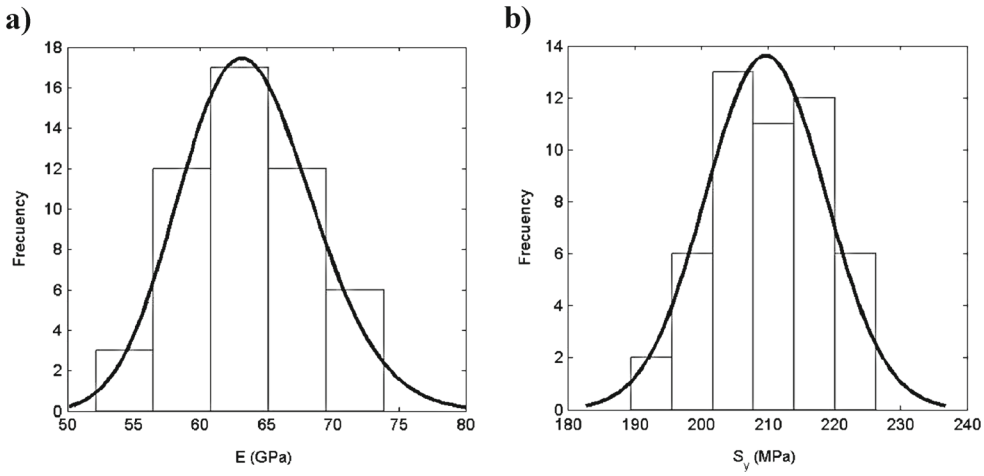

Fig. 4 Frequency histogram of mechanical properties, (**a**) Young's modulus (E), (**b**) yield strength (S_y)

function as the surrogate models under consideration; as discussed in Jin et al. (2001), Song et al. (2010) and Song et al. (2013), using multiple surrogates give us a rationale for surrogate model selection. A data set of 1320 samples was generated using the Latin hypercube sampling (LHS) procedure (McKay et al. 1979) available in MATLAB® through the lhsdesign command; the sample size was obtained as the maximum among the recommended minimum sample size for polynomial regression (Lian and Liou 2006), Kriging (Jones et al. 1998) and radial basis functions (Barton and Meckesheimer 2006). The M and, S_{max} and f_{buck} values associated with each of the samples in the DOE were determined using mass property analysis, and FE numerical simulations in the ANSYS Workbench®, respectively. Using 10-fold cross-validation, prediction errors, such as percentage maximum absolute error (MAXE%), percentage root mean square error (RMSE%), the coefficient of determination (R^2) and relative errors (Error) were estimated for each of the surrogate-models under consideration.

A brief description of each of the surrogate models under consideration is next.

A. Polynomial regression (PRG)

In this work the regression models (Draper and Smith 1969) considered are of linear (L),

Table 3 Probability distributions of Al 6063-T5 material properties

Material properties	Unit	Probability distribution	Mean value	Characteristic value (5%)
Density (ρ)	Kg/m^3	Fixed	2700	–
Young's modulus (E)	MPa	LN(11.059, 0.0709)	63,657.5	55,805.866
Yield strength (S_y)	MPa	N(209.69,9.002)	209.69	194.883
Poisson's ratio (ν)	–	Fixed	0.33	–

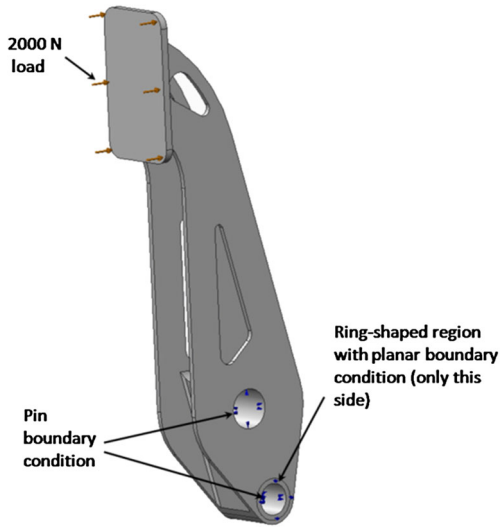

Fig. 5 Structural analysis domain with applied load and boundary conditions of the FSAE brake pedal numerical model

$$\hat{y}(\mathbf{x}) = \beta_0 + \sum_{i=1}^{n_{rv}} \beta_i x_i \tag{7}$$

and quadratic form (Q):

$$\hat{y}(\mathbf{x}) = \beta_0 + \sum_{i=1}^{n_{rv}} \beta_i x_i + \sum_{i=1}^{n_{rv}} \beta_{ii} x_{ii}^2 + \sum_{i=1}^{n_{rv}-1} \sum_{j=i+1}^{n_{rv}} \beta_{ij} x_i x_j \tag{8}$$

where n_{rv} is the total number of random variables, x_i, and the parameters β_0, β_i, β_{ii} and β_{ij} are estimated by the least-squares method implemented in MATLAB® (regress command).

B. Kriging model (KRG)

A Kriging model (Sacks et al. 1989) postulates a combination of a polynomial model f(**x**) and an error model of the form, Z(**x**) as:

Table 5 FSAE brake pedal design variables values for initial model

Design variable	Values (mm)	Design variable	Values (mm)
d1	27	d10	3
d2	80	d11	12
d3	70	d12	110
d4	8	d13	5
d5	3	d14	60
d6	12	d15	4
d7	6	d16	67
d8	5	d17	4
d9	10	d18	2.2

$$\hat{y}(\mathbf{x}) = f(\mathbf{x}) + Z(\mathbf{x}) \tag{9}$$

where $y(\mathbf{x})$ is the unknown function of interest, f(**x**) is the regression function of **x** and Z(**x**) is a random function (stochastic process) with mean zero, and nonzero covariance given by the following expression:

$$\mathrm{Cov}\left[Z(x_i, x_j)\right] = \sigma^2 \mathbf{R}(x_i, x_j) \tag{10}$$

Where, σ^2 is the process variance and **R** is the correlation function. In this work, consideration is given to constant (0) and linear (1) regression functions, and Gaussian (G), exponential (E), linear (L) and spherical (S) correlation functions. The parameters of correlation and regression functions are identified using a maximum likelihood estimator. The Kriging models were implemented using Design and Analysis Computational Experiments (DACE) toolbox developed by Lophaven et al. (2002) and available in MATLAB®.

C. Radial basis function (RBF)

Radial basis function surrogate models (Hardy 1971) are constructed using a linear combination of radially symmetric functions evaluated with Euclidean distances of the form,

Table 4 S_{max} and f_{buck} errors vs. computational time (CT) for different finite element maximum lengths in the brake pedal numerical model

Finite element maximum length (mm)	Number of elements	S_{max} (MPa)	Relative error (%)	CT (seg)	f_{buck}	Relative error (%)	CT (seg)	Total CT (seg)
Default mesh	2949	194.67	2.200	4	1.3269	13.043	5	9
8	2923	197.51	0.774	4	1.2611	7.437	4	8
7	2568	195.83	1.618	4	1.3200	12.455	4	8
6	2981	196.89	1.085	4	1.2868	9.627	6	10
5	3658	197.25	0.904	3	1.2660	7.855	6	9
4	4521	196.07	1.497	4	1.2417	5.785	6	10
3	7555	197.96	0.548	6	1.2053	2.684	7	13
2	14,558	198.54	0.256	9	1.1855	0.997	18	27
1	67,804	199.05	0.000	29	1.1738	0.000	1120	1149

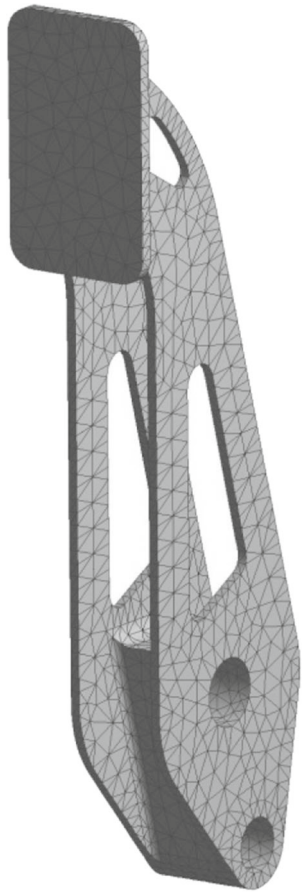

Fig. 6 Mesh grid for FSAE brake pedal model (initial model, 129.45 g) with a maximum length of 3 mm for tetrahedral elements (number of elements = 7555)

$$\hat{y}(\mathbf{x}) = \sum_{i=1}^{n} \lambda_i \phi(\|\mathbf{x}\text{-}\mathbf{x_i}\|) \tag{11}$$

where, n is the number of the sample points, $\mathbf{x}$ is the input variable vector, $\mathbf{x_i}$ is the vector of the input variable at the ith sample point, $\|.\|$ is the Euclidean norm, ϕ is a basis function, and λ_i is the coefficient of the basis function. In this work, the basis functions given consideration are: Gaussian (G), linear (L), cubic (C), multi-quadratic (MQ), inverse multi-quadratic (IMQ) and thin plate spline (TPS). The unknown parameters of RBFs are obtained from the solution of a system of linear equations. The radial basis functions were implemented using the MATSUMOTO toolbox in MATLAB® by Mueller (2014).

5 Global sensitivity analysis and surrogate models selection

A significant reduction of the number of random variables under consideration (43), could be obtained through a global sensitivity analysis for the functions M, S_{max} and f_{buck} (Sobol 2001; Carrero et al. 2007), which may improve the surrogate models effectiveness, i.e., accuracy and computational cost. The main factor sensitivity index (S_i) represents the relative contribution of random variable i to the total function variance and is calculated as:

$$S_i = \frac{V_i}{V} \tag{12}$$

with partial variance of random variable i, V_i and total variance V computed as follows:

$$V_i = \frac{1}{n}\sum_{p=1}^{n}\left[f(\xi_p) f\left(\xi_p^{'i}\right)\right] - f_0^2; \quad i = 1, 2, 3, \ldots, n \tag{13}$$

$$f_0 = \frac{1}{n}\sum_{p=1}^{n} f(\xi_p) \tag{14}$$

$$V = \frac{1}{n}\sum_{p=1}^{n}\left[f(\xi_p)\right]^2 - f_0^2 \tag{15}$$

On the other hand, the second and third order sensitivity indices are calculated as:

$$S_{ij} = \frac{V_{ij}}{V} \tag{16}$$

$$S_{ijk} = \frac{V_{ijk}}{V} \tag{17}$$

with partial variances of interaction effects V_{ij} and V_{ijk}, calculated as (Mack et al. 2005):

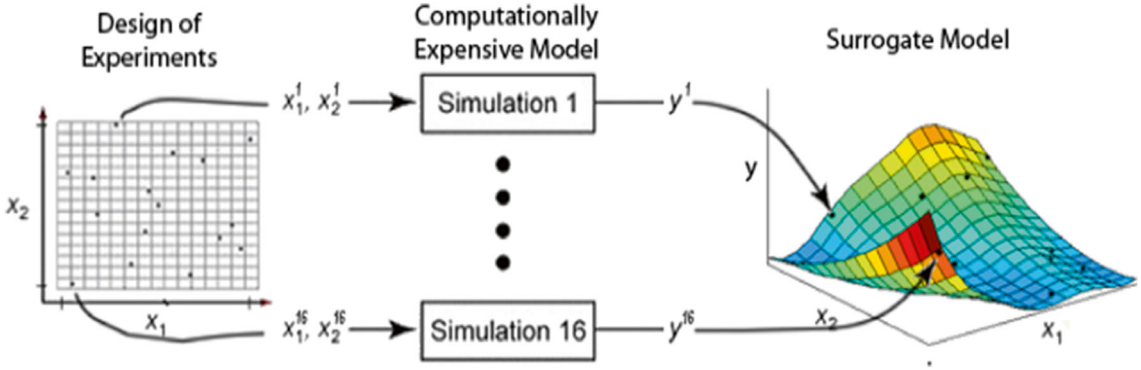

Fig. 7 Basic steps of the surrogate-based modeling approach for a 3D function

$$V_{ij} = \frac{1}{n}\sum_{p=1}^{n}\left[f(\xi_p)\, f\left(\xi_p'^{ij}\right)\right] - f_0^2 - V_i - V_j;\quad i = 1,2,3\ldots,n;\quad j > i \tag{18}$$

$$V_{ijk} = \frac{1}{n}\sum_{p=1}^{n}\left[f(\xi_p)\, f\left(\xi_p'^{ijk}\right)\right] - f_0^2 - V_{ij} - V_{ik} - V_{jk} - V_i - V_j - V_k;\ldots \quad i = 1,2,3,\ldots,n;\quad j > i;\quad k > j \tag{19}$$

Under the independent model inputs assumption, the sum of the sensitivity indices must be equal to one. To calculate the total sensitivity index (S_{itotal}) of a random variable i, the random variable vector $\mathbf{x}$ is divided into two complementary subsets, x_i and $\mathbf{Z}_i$ where $\mathbf{Z}_i$ is a vector containing x_1, x_2, x_3, …, x_n ($n \neq i$). The purpose of using these subsets is to isolate the influence of x_i on the f(x) variability from the influence of the remaining design variables included in $\mathbf{Z}_i$. The total sensitivity index for x_i is then computed as:

$$S_{itotal} = \frac{V - V_{zi}}{V} \tag{20}$$

If interaction effects are not significant ($S_{itotal} \approx S_i$), random variables with main factor sensitivity indices below a given threshold can be labeled as deterministic (at their mean value) and a reduced set of design variables and parameters can be obtained. Then, the surrogate models are updated using the reduced set of design variables and parameters, and a single surrogate model for each of the functions of interest M, S_{max} and f_{buck} is selected based on performance measures such as, local and global error, and computational time. Each of the surrogate relative error probability distribution was estimated as, $\varepsilon = N(\mu_{Error}, \sigma_{Error})$.

6 Surrogate-based RBDO and DDO with risk allocation analysis

6.1 Risk allocation analysis in RBDO and DDO

Figure 8 shows the procedure used to conduct the risk allocation analysis in RBDO and DDO. First, a brake pedal deterministic optimization (DDO) was conducted for safety factors in the interval (1, 2.125) with the probability of system failure P(F) estimated using Monte Carlo simulation (MCS). Then, for each of the DDO probability of system failure a reliability-based design optimizations is conducted. Finally, risks associated for each of the failure modes in RBDO and DDO are analyzed.

6.2 Brake pedal DDO and probability of system failure

The brake pedal DDO problem (1, 3, 4) is solved using sequential quadratic programming (SQP) (Powell 1978) as implemented in the MATLAB® fmincon command with randomly selected starting points (20). The probability of failure

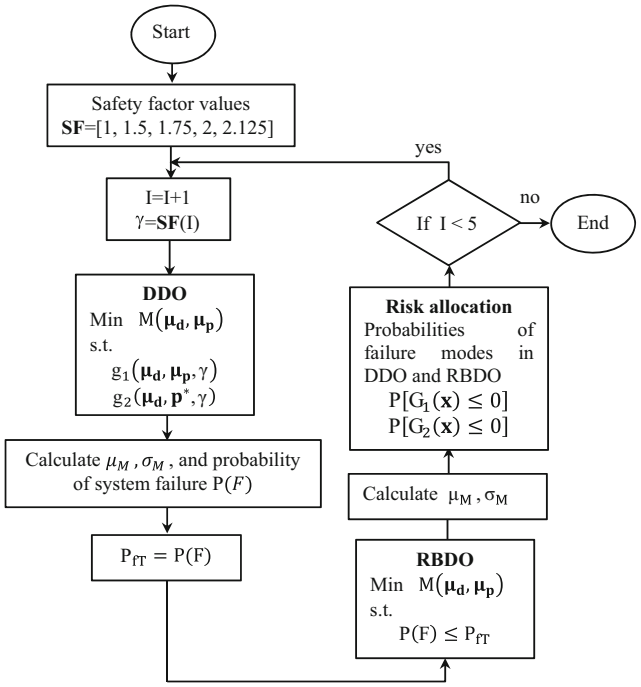

Fig. 8 Risk allocation procedure for the FSAE brake pedal

for failure mode j was estimated using Monte Carlo simulations (MCS) (Rubinstein 1981) as:

$$P(F_j) \approx \frac{1}{n}\sum_{i=1}^{n} I\left[G_j(\mathbf{x_i}) < 0\right] \tag{21}$$

where, $\mathbf{x_i}$ is a vector of the input variable at the ith sample point, n is the total number of samples, $G_j(\mathbf{x_i})$ is the limit state function for failure mode j, and I is the indicator function, which equals 1 if the condition is true and 0 if the condition is false. The accuracy of MCS largely depends on the number of simulation cycles and for this scenario has been taken equal to 10^7. In this context, the $\mathbf{x_i}$ realizations are the result of sampling probability distributions for the random parameters (Table 2) and design variables, with the latter specified as, $d_i = \mu_{d_i} + tol_i$, where μ_{d_i} represents the design variable i mean value (obtained from the solution of the DDO problem) and tol_i denotes the manufacturing tolerance probability distribution of d_i (Table 1).

Since two failure modes (stress and buckling condition) are accounted for, a system reliability approach is necessary for estimating the probability of failure for the brake pedal design under consideration. In this case, system failure occurs when any of the failure modes is active, hence it is referred to as a series system (or a weak link system) and defined as the probability of the union of the individual failure modes (Haldar and Mahadevan 2000) as shown below:

$$P(F) = P[G_1(\mathbf{d},\mathbf{p}) \leq 0 \cup G_2(\mathbf{d},\mathbf{p}) \leq 0]$$
$$= P[G_1(\mathbf{d},\mathbf{p}) \leq 0] + P[G_2(\mathbf{d},\mathbf{p}) \leq 0] - P[G_1(\mathbf{d},\mathbf{p}) \leq 0 \cap G_2(\mathbf{d},\mathbf{p}) \leq 0] \tag{22}$$

Table 6 Surrogate models M, S_{max} and f_{buck} ten-fold cross-validation prediction errors, namely, percentage maximum absolute error (MAXE%), percentage root mean square error (RMSE%) and the coefficient of determination (R^2); in bold surrogate models with the best performance

Surrogate model	M				S_{max}				f_{buck}			
	MAXE%	RMSE%	R2	t_f(s)	MAXE%	RMSE%	R2	t_f(s)	MAXE%	RMSE%	R2	t_f(s)
KRG_G0	24.209	6.168	0.941	1516.35	83.181	15.884	0.878	1689.72	100.274	25.147	0.904	1513.48
KRG_G1	3.092	0.649	0.999	1905.29	66.357	11.917	0.930	1858.29	38.523	8.837	0.987	1872.51
KRG_E0	6.480	1.664	0.995	1731.73	60.325	11.741	0.933	1729.24	45.786	9.729	0.985	1722.34
KRG_E1	2.522	0.556	0.999	2030.84	58.744	10.831	0.942	2039.01	**28.345**	**5.704**	**0.995**	**2061.61**
KRG_L0	6.715	1.774	0.994	1833.99	60.647	11.833	0.932	1811.53	47.752	10.229	0.983	1817.98
KRG_L1	2.637	0.584	0.999	2067.83	**56.607**	**10.491**	**0.946**	**2111.26**	29.017	5.822	0.994	2075.87
KRG_S0	10.919	2.785	0.986	2063.91	73.560	13.961	0.906	2050.48	69.931	16.417	0.956	2036.19
KRG_S1	3.031	0.685	0.999	2195.68	61.599	11.788	0.932	2247.61	35.518	7.383	0.991	2317.78
PRG_L	7.359	2.204	0.991	0.222	86.694	19.887	0.805	0.197	71.073	20.194	0.933	0.214
PRG_Q	**1.262**	**0.415**	**1.000**	**3.210**	67.908	21.131	0.802	3.556	23.957	8.262	0.989	3.494
RBF_G	7.336	2.205	0.991	1.808	87.869	19.932	0.804	1.369	70.716	20.269	0.933	1.319
RBF_L	8.163	2.553	0.988	1.217	97.794	22.904	0.746	1.285	74.696	22.716	0.916	1.214
RBF_C	10.312	3.292	0.980	1.899	116.937	30.333	0.606	1.948	83.245	27.349	0.882	1.899
RBF_MQ	8.178	2.561	0.988	1.283	98.115	22.983	0.745	1.321	74.734	22.780	0.915	1.404
RBF_MQI	7.323	2.209	0.991	1.303	88.151	19.962	0.803	1.332	71.112	20.239	0.933	1.316
RBF_TPS	8.860	2.839	0.985	1.444	109.024	25.818	0.690	1.513	73.269	23.966	0.907	1.480

Table 7 Main factor variances and relative variances considering an initial brake pedal design and set of surrogate models; in bold random parameter/variable with relative variance higher than a given threshold (0.5%)

Random parameter/ variable	M		S_{max}		f_{buck}		Random parameter/ variable	M		S_{max}		f_{buck}	
	V_i	S_i (%)	V_i	S_i (%)	V_i	S_i (%)		V_i	S_i (%)	V_i	S_i (%)	V_i	S_i (%)
d1	47.872	**1.841**	91.630	**5.122**	0.353	0.440	c5	4.154	0.160	2.300	0.129	0.054	0.067
d2	41.141	**1.582**	13.986	**0.782**	0.358	0.446	c6	3.330	0.128	2.263	0.126	0.056	0.069
d3	72.282	**2.779**	18.458	**1.032**	0.669	**0.833**	c7	3.845	0.148	2.520	0.141	0.053	0.066
d4	10.219	0.393	5.851	0.327	0.083	0.104	c8	3.527	0.136	2.469	0.138	0.054	0.067
d5	19.193	**0.738**	2.074	0.116	0.108	0.135	c9	3.465	0.133	2.522	0.141	0.054	0.067
d6	3.332	0.128	2.424	0.136	0.052	0.064	c10	3.287	0.126	2.500	0.140	0.053	0.066
d7	5.861	0.225	1.807	0.101	0.067	0.083	c11	3.216	0.124	2.349	0.131	0.061	0.076
d8	3.283	0.126	1.973	0.110	0.056	0.069	c12	3.471	0.133	2.336	0.131	0.066	0.082
d9	4.448	0.171	0.157	0.009	0.058	0.072	c13	3.280	0.126	2.541	0.142	0.053	0.066
d10	3.589	0.138	1.637	0.092	0.059	0.073	c14	3.272	0.126	2.505	0.140	0.054	0.067
d11	3.297	0.127	28.403	**1.588**	0.163	0.203	c15	3.586	0.138	2.395	0.134	0.063	0.078
d12	25.579	**0.983**	60.698	**3.393**	1.132	**1.409**	c16	3.439	0.132	2.526	0.141	0.058	0.072
d13	7.414	0.285	18.399	**1.029**	0.247	0.307	c17	3.249	0.125	2.532	0.142	0.053	0.066
d14	4.212	0.162	1.969	0.110	0.084	0.105	c18	3.327	0.128	2.540	0.142	0.066	0.082
d15	3.372	0.130	2.313	0.129	0.054	0.067	c19	3.346	0.129	2.549	0.142	0.053	0.066
d16	4.475	0.172	0.796	0.044	0.082	0.102	c20	3.294	0.127	2.415	0.135	0.054	0.067
d17	3.216	0.124	2.311	0.129	0.054	0.067	c21	3.268	0.126	2.489	0.139	0.054	0.067
d18	1127.626	**43.356**	572.284	**31.992**	33.517	**41.724**	c22	3.550	0.137	2.528	0.141	0.055	0.068
c1	3.270	0.126	2.467	0.138	0.053	0.066	**c23**	1113.880	**42.827**	745.343	**41.667**	33.235	**41.373**
c2	3.275	0.126	2.495	0.139	0.053	0.066	c24	3.279	0.126	2.519	0.141	0.053	0.066
c3	3.268	0.126	2.543	0.142	0.054	0.067	**E**	3277	0.126	2.447	0.137	1520	**1.893**
c4	3.294	0.127	2.410	0.135	0.054	0.067							

Table 8 Surrogate models M, S_{max} and f_{buck} ten-fold cross-validation prediction errors with essential random variables; in bold surrogate models with the best compromise between accurate and computational effort

Surrogate Model	M				S_{max}				f_{buck}			
	MAXE%	RMSE%	R2	t_f(s)	MAXE%	RMSE%	R2	t_f(s)	MAXE%	RMSE%	R2	t_f(s)
KRG_G0	0.079	0.023	1.000	2.419	22.772	7.007	0.962	2.944	5.354	1.359	1.000	3.194
KRG_G1	0.682	0.203	1.000	3.148	22.077	6.336	0.968	3.113	5.505	1.538	1.000	3.412
KRG_E0	1.673	0.508	0.999	3.174	23.095	6.218	0.972	3.059	16.941	4.403	0.996	3.173
KRG_E1	1.224	0.348	1.000	3.152	22.352	5.801	0.975	3.204	16.014	4.078	0.997	3.242
KRG_L0	1.521	0.444	1.000	3.175	21.924	5.910	0.973	2.921	15.147	4.038	0.997	3.345
KRG_L1	1.259	0.399	1.000	3.297	21.291	5.717	0.975	3.105	13.796	3.601	0.998	3.316
KRG_S0	1.875	0.529	0.999	3.592	22.194	6.098	0.973	3.460	18.171	4.999	0.995	3.561
KRG_S1	1.003	0.273	1.000	3.475	22.300	5.925	0.974	3.320	15.161	4.035	0.997	3.240
PRG_L	5.468	1.781	0.993	0.002	41.680	13.528	0.872	0.002	50.084	17.341	0.944	0.002
PRG_Q	**0.534**	**0.172**	**1.000**	**0.009**	**21.005**	**6.134**	**0.971**	**0.008**	**10.188**	**3.516**	**0.998**	**0.008**
RBF_G	5.468	1.781	0.993	0.017	41.680	13.528	0.872	0.014	50.084	17.341	0.944	0.013
RBF_L	5.767	2.078	0.990	0.012	52.944	17.370	0.798	0.014	60.352	22.092	0.908	0.013
RBF_C	7.680	2.620	0.984	0.022	69.026	24.486	0.656	0.023	64.644	25.976	0.876	0.022
RBF_MQ	5.795	2.084	0.990	0.014	53.159	17.438	0.796	0.016	60.553	22.168	0.907	0.015
RBF_MQI	5.437	1.777	0.993	0.014	41.804	13.556	0.872	0.014	50.245	17.401	0.943	0.014
RBF_TPS	6.696	2.322	0.987	0.019	60.455	20.376	0.738	0.019	64.796	23.707	0.894	0.016

6.3 Brake pedal probabilistic optimization (RBDO)

The brake pedal RBDO problem (1, 2, 5, 6) was solved with the same optimization approach used for the corresponding DDO, but with significantly higher search starting points (800) to ensure convergence. The RBDO solutions with highest probability of failure, corresponding to the first three DDO designs (SFs: 1, 1.5, 1.75), were obtained with 10^5 MC simulation cycles, and the last two (SFs: 2, 2.125) with 10^6 cycles; once obtained the RBDO solutions, the probabilities for the failure modes and the system failure are evaluated with 10^7 simulation cycles to ensure the accuracy of the results.

In this work, unbiased estimators of the mean value, and standard deviation of the random brake pedal mass function M $(\mathbf{x})$ were obtained using the MCS method with 10^5 simulation cycles (Papadrakakis and Lagaros 2002):

$$\mu_M \approx \frac{1}{n}\sum_{i=1}^{n}\hat{M}(\mathbf{x_i}) \tag{23}$$

$$\sigma_M \approx \sqrt{\frac{1}{n\text{-}1}\sum_{i=1}^{n}\left[\hat{M}(\mathbf{x_i})-\mu_M\right]^2} \tag{24}$$

with $\mathbf{x_i}$ being vector of the input variable at the ith sample point, n is the total number of samples, $\hat{M}(\mathbf{x_i}) = M(\mathbf{x_i})\ (1+\varepsilon_{Mi})$, and $M(\mathbf{x})$ and ε_M denoting the mass surrogate model, and surrogate relative error probability distribution, respectively.

7 Results and discussion

This section shows the results of: surrogate modeling of mass, maximum von Mises stress and buckling load factor, global sensitivity analysis and surrogate model selection, deterministic and reliability-based brake pedal design optimization and risk allocation analysis in DDO and RBDO.

When considering the mass surrogate model (M), quadratic Regression showed the best performance (Table 6). On the other hand, for the S_{max} and f_{buck} surrogate models, Kriging with linear correlation and linear regression (KRG_L1) and Kriging with exponential correlation and linear regression (KRG_E1) gave the best results, respectively. The best surrogate model was considered the one with the lowest values for MAXE%, and RMSE% and the highest R^2 using 10-fold cross-validation prediction errors. Considering significant errors were observed, a global sensitivity analysis was scheduled to potentially reduce the number of parameters and variables and hence help improve the surrogate models accuracy.

Table 9 Normal probability distribution parameters of surrogate model errors

Surrogate model error	Normal distribution	
	μ	σ
ε_M	-0.0000001	0.0019
ε_S	-0.0019	0.0606
ε_b	-0.0012	0.1442

Table 10 Deterministic brake pedal optimal designs considering alternative safety factors with probability of failure modes, mass mean and standard deviation, computational time (CT) and, mass, S_{max}, and f_{buck} numerically calculated values

Parameter	Unit	Safety factor				
		1	1.5	1.75	2	2.125
μ_{d_1}	mm	30.926	30.156	33.000	33.000	33.000
μ_{d_2}	mm	80.000	78.607	79.607	79.327	78.859
μ_{d_3}	mm	70.000	75.745	87.000	87.000	87.000
μ_{d_5}	mm	2.000	2.000	2.000	2.000	2.000
$\mu_{d_{11}}$	mm	15.545	17.412	17.903	17.118	16.811
$\mu_{d_{12}}$	mm	115.000	80.000	80.000	80.000	80.000
$\mu_{d_{13}}$	mm	6.868	3.111	6.815	5.095	4.488
$\mu_{d_{18}}$	mm	2.000	2.000	2.032	2.337	2.481
$P[G1(\mathbf{x}) \leq 0]$	–	0.2068	0	0	0	0
$P[G2(\mathbf{x}) \leq 0]$	–	0.964394	0.318518	0.046325	0.0003074	0.0000136
P(F)	–	0.974229	0.318518	0.046325	0.0003074	0.0000136
$\mu_M(\mathbf{x})$	g	122.897	137.932	149.871	163.151	169.852
$\sigma_M(\mathbf{x})$	g	3.795	4.623	5.133	5.258	5.325
CT	s	32	34	32	31	32
$M(\mu_x, \mu_p)_{ANSYS}$	g	123.953	138.682	149.636	163.496	170.355
$S_{max}(\mu_x, \mu_p)_{ANSYS}$	MPa	268.923	124.779	105.936	89.761	84.442
$f_{buck}(\mu_x, p^*)_{ANSYS}$	–	0.583	1.304	1.477	2.259	2.705

Table 11 RBDO brake pedal optimal designs for DDO probability of system failures (targets), with probability of failure modes, mass mean and standard deviation, computational time (CT) and, mass, S_{max}, and f_{buck} numerically calculated values

Parameter	Unit	Target probability of system failure (P_{fT})				
		0.974229	0.318518	0.046325	0.0003074	0.0000136
μ_{d_1}	mm	27.000	27.000	27.005	27.327	27.204
μ_{d_2}	mm	80.000	79.998	79.951	79.657	79.756
μ_{d_3}	mm	70.005	70.000	70.953	70.986	71.211
μ_{d_5}	mm	2.000	2.000	2.002	2.070	2.046
$\mu_{d_{11}}$	mm	11.821	13.488	14.208	16.075	16.437
$\mu_{d_{12}}$	mm	115.000	107.799	83.367	85.108	83.131
$\mu_{d_{13}}$	mm	6.840	4.078	5.490	4.927	3.931
$\mu_{d_{18}}$	mm	2.000	2.000	2.007	2.337	2.422
$P[G1(\mathbf{x}) \leq 0]$	–	0.9221510	0.2079706	0.0083576	0.0000356	0.0000017
$P[G2(\mathbf{x}) \leq 0]$	–	0.6378130	0.1451721	0.0384367	0.0002724	0.0000120
P(F)	–	0.974	0.31852	0.046326	0.000308	0.0000137
$\mu_M(\mathbf{x})$	g	116.998	123.581	128.307	139.387	142.461
$\sigma_M(\mathbf{x})$	g	3.426	3.636	3.877	3.953	4.022
CT	s	53,861	55,775	56,386	511,861	533,498
$M(\mu_x, \mu_p)_{ANSYS}$	g	117.899	123.157	127.620	139.036	142.434
$S_{max}(\mu_x, \mu_p)_{ANSYS}$	MPa	284.732	192.316	164.230	154.673	143.966
$f_{buck}(\mu_x, p^*)_{ANSYS}$	–	0.623	0.891	1.096	1.700	1.945

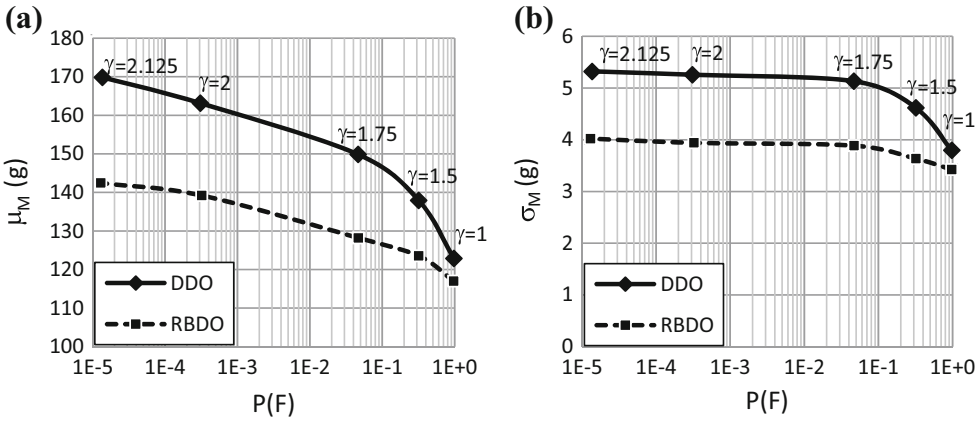

Fig. 9 Brake pedal mass mean (**a**) and standard deviation (**b**) vs. probability of system failure considering alternative safety factors

For the M, S_{max} and f_{buck} surrogate models the contribution of the main factor variances to the total variance are 99.423%, 91.215% and 91.164%, respectively, which suggests interaction effects are not significant in this particular case. Results show that when the main factors with relative variances (S_i) lower than 0.5% are filtered out, only eight out of eighteen random design variables, i.e., d1, d2, d3, d5, d11, d12, d13 and d18 and two out of twenty five random parameters, i.e., c23, E should be accounted for (Table 7).

Considering the significant reduction of random parameters and design variables (now only 10 random variables) a new set of surrogate models was constructed. To improve the surrogate modeling accuracy the DOE included 500 experiments, well above the recommended minimum (Lian and Liou 2006; Jones et al. 1998; Barton and Meckesheimer 2006). In this new scenario, while Kriging methods showed the best performance (lowest MAXE% and RMSE%, and highest R^2) among all surrogates for mass (M), S_{max} and f_{buck} (Table 8), quadratic regression provided the best compromise solution considering prediction error measures and computing time. Hence, quadratic regression was selected for all instances to obtain accurate DDO and RBDO solutions with reasonable computational effort. Table 9 shows the error distribution parameters for all surrogate models under consideration.

When considering the same DDO probability of system failure (and all safety factors), the RBDO brake pedals exhibits (Tables 10 and 11): significant reductions in the design variables d1 and d3, on average 15.22% and 12.52%, respectively. In addition, it depicts a 12.06% average mass reduction (Fig. 9), and a more balanced allocation of risk, i.e., DDO in most cases fails exclusively by buckling. Specifically, Fig. 10 shows the shape differences between RBDO and DDO brake pedals with a probability of system failure of 0.000308 (safety factor equal to 2), with the former brake pedal exhibiting, 17% and 18% smaller d1 and d3, respectively, a 14.5% mass reduction with 25% less variability for the cases of practical interest, and the stress probability of failure, $P[G1(\mathbf{x}) \leq 0] = 0.0000356$ (vs. 0 for DDO).

Figure 11 shows the more balanced risk allocation of RBDO versus the DDO for all safety factors. Using as performance measure the difference of the ratio of the spread of probabilities of failure modes (stress and buckling) and system failure for RBDO and DDO, the RBDO results show minimum, maximum and average improvements of 22.89%, 80.28% and 42.04%, respectively.

8 Conclusions

This work solved RBDO and DDO models with multiple failure modes (stress and buckling) of a FSAE brake pedal with their relative performance evaluated through a risk allocation analysis. The brake pedal design under uncertainty of FSAE vehicles represents an easy to understand structural problem among engineering students and practitioners, and an opportunity to highlight the potential of achieving

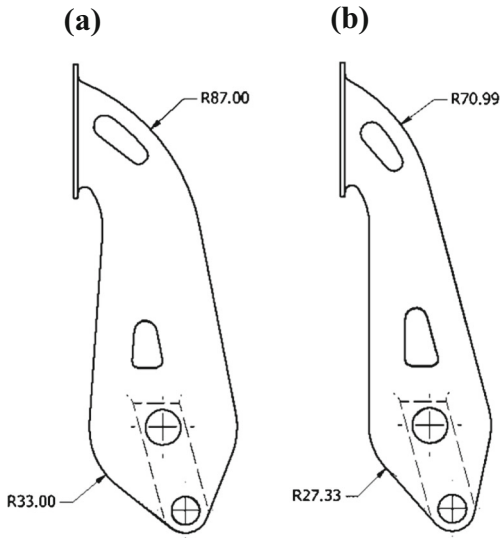

Fig. 10 DDO (**a**) and RBDO (**b**) brake pedal shapes for a given probability of failure (P(F) = 0.000308) with indication of design variables with most significant differences

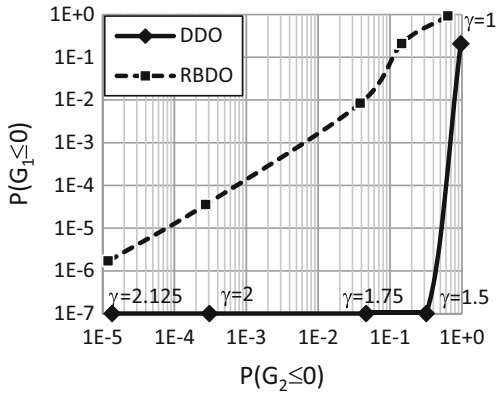

Fig. 11 Probability of failures considering stress ($P[G_1(\mathbf{x}) \leq 0]$) and buckling failure modes ($P[G_2(\mathbf{x}) \leq 0]$) for alternative safety factors (γ)

significant weight savings and more robust designs by balancing the risks among failure modes through RBDO.

When compared to DDO with alternative safety factors, for the same probability of system failure, the RBDO brake pedal designs were significantly lighter and more robust (less mass variability). Future work will evaluate uncertainty reduction measures at each level of the product life cycle (pre-design, design and post-design) and their impact on RBDO and risk allocation among failure modes.

References

Acar E, Haftka RT (2007) Reliability–based aircraft structural design pays, even with limited statistical data. J Aircr 44(3):812–823

Acar E, Solanki K (2009) System reliability based vehicle design for crashworthiness and effects of various uncertainty reduction measures. Struct Multidiscip Optim 39(3):311–325

Acar E, Haftka RT, Kim NH (2010) Effects of structural tests on aircraft safety. AIAA J 48(10):2235–2248

Allison DL, Morris CC, Schetz JA, Kapania RK, Watson LT, Deaton JD (2015) Development of a multidisciplinary design optimization framework for an efficient supersonic air vehicle. Advances in Aircraft and Spacecraft Science 2(1):17–44

ASME (2016) ASME competitions. https://www.asme.org/events/competitions

ASTM (2007) B557M-07 - Standard test methods for tension testing wrought and cast aluminum- and magnesium-alloy products (Metric). ASTM

Barroso L (2015) Propuesta de un modelo estocástico para la determinación de las propiedades dinámicas del aluminio 6063-T5. Master dissertation. Universidad del Zulia

Barton RR, Meckesheimer M (2006) Metamodel-based simulation optimization. Handbooks in Operations Research and Management Science 13:535–574

Beck AT, de Santana Gomes WJ (2012) A comparison of deterministic, reliability-based and risk-based structural optimization under uncertainty. Probabilistic Engineering Mechanics 28:18–29

Bendsoe MP, Kikuchi N (1988) Generating optimal topologies in structural design using a homogenization method. Comput Methods Appl Mech Eng 71(2):197–224

Carrero E, Queipo NV, Pintos S, Zerpa LE (2007) Global sensitivity analysis of alkali–surfactant–polymer enhanced oil recovery processes. J Pet Sci Eng 58(1):30–42

D'Agostino RB (1986) Goodness-of-fit-techniques. CRC press 68

Deb A, Gunti RS, Chou C, Dutta U (2015) Use of truncated finite element modeling for efficient design optimization of an automotive front end structure. SAE Int J, SAE Technical Paper No. 2015–01-0496

Draper N, Smith H (1969) Applied regression analysis. Biom J 11(6):427–427

Forrester A, Keane A (2009) Recent advances in surrogate-based optimization. Prog Aerosp Sci 45(1–3):50–79

Frangopol DM (1985) Structural optimization using reliability concepts. J Struct Eng 111(11):2288–2301

Gern FH (2015) Update on HCDstruct-a tool for hybrid wing body conceptual design and structural optimization. In: 15th AIAA aviation technology, integration, and operations conference, Dallas, June. AIAA Paper No. 2544

Gu X, Sun G, Li G, Mao L, Li Q (2013) A comparative study on multiobjective reliable and robust optimization for crashworthiness design of vehicle structure. Struct Multidiscip Optim 48(3):669–684

Haldar A, Mahadevan S (2000) Probability, reliability and statistical methods in engineering design. Wiley, New York

Han ZH, Zhang KS (2012) Surrogate-based optimization. Intec book, real-world application of genetic algorithm. InTech, pp 343-362

Hardy RL (1971) Multiquadric equations of topography and other irregular surfaces. J Geophys Res 76(8):1905–1915

ISO (1989) ISO 2768–1 - General tolerances - Part 1: tolerances for linear and angular dimensions without individual tolerance indications. International Organization for Standardization

Jin R, Chen W, Simpson TW (2001) Comparative studies of metamodelling techniques under multiple modelling criteria. Struct Multidiscip Optim 23(1):1–13

Jones D, Schonlau M, Welch W (1998) Efficient global optimization of expensive black-box functions. J Glob Optim 13(4):455–492

Lee SJ (1987) Reliability based design optimization. PhD dissertation. The University of Arizona

Lian Y, Kim NH (2006) Reliability-based design optimization of a transonic compressor. AIAA J 44(2):368–375

Lian Y, Liou MS (2006) Aerostructural optimization of a transonic compressor rotor. J Propuls Power 22(4):880–888

Liu K, Tovar A (2014) An efficient 3D topology optimization code written in Matlab. Struct Multidiscip Optim 50(6):1175–1196

Liu D, Toropov VV, Barton DC, Querin OM (2015) Weight and mechanical performance optimization of blended composite wing panels using lamination parameters. Struct Multidiscip Optim 52(3):549–562

Lophaven SN, Nielsen HB, Søndergaard J (2002) Aspects of the DACE MATLAB Toolbox. IMM, Technical University of Denmark, KongensLyngby

Lyu Z, Martins JR (2015) Aerodynamic shape optimization of an adaptive morphing trailing-edge wing. J Aircr 52(6):1951–1970

Mack Y, Goel T, Shyy W, Haftka R, Queipo N (2005) Multiple surrogates for the shape optimization of bluff body-facilitated mixing. 43rd AIAA aerospace sciences meeting and exhibit, Reno, NV, Jan 10–13. AIAA-2005-0333

Mårtensson P, Zenkert D, Åkermo M (2015) Effects of manufacturing constraints on the cost and weight efficiency of integral and differential automotive composite structures. Compos Struct 134:572–578

McKay M, Bechman R, Conover W (1979) Comparison of three methods for selecting values of input variables in the analysis of output from a computer code. Technometrics 21(2):239–245

Mlejnek HP (1992) Some aspects of the genesis of structures. Structural Optimization 5(1–2):64–69

Mueller J (2014) MATSuMoTo: The MATLAB Surrogate Model Toolbox for Computationally Expensive Black-Box Global Optimization Problems. arXiv:1404.4261

Neufeld D, Behdinan K, Chung J (2010) Aircraft wing box optimization considering uncertainty in surrogate models. Struct Multidiscip Optim 42(5):745–753

Papadrakakis M, Lagaros ND (2002) Reliability-based structural optimization using neural networks and Monte Carlo simulation. Comput Methods Appl Mech Eng 191(32):3491–3507

Papadrakakis M, Lagaros ND, Plevris V (2005) Design optimization of steel structures considering uncertainties. Eng Struct 27(9):1408–1418

Plšek J, Štepánek P, Popela P (2007) Deterministic and reliability based structural optimization of concrete cross-section. J Adv Concr Technol 5(1):63–74

Powell MJD (1978) A fast algorithm for nonlinear constrained optimization calculations. Mathematics 630:144–157

Qu X, Haftka RT, Venkataraman S, Johnson TF (2003) Deterministic and reliability-based optimization of composite laminates for cryogenic environments. AIAA J 41(10):2029–2036

Queipo N, Haftka RT, Shyy W, Goel T, Vaidyanathan R, Tucker PK (2005) Surrogate-based analysis and optimization. Prog Aerosp Sci 41(1):1–28

Rangavajhala S, Liang C, Mahadevan S (2012) Design optimization under aleatory and epistemic uncertainties. In: Proceedings of 14th AIAA/ISSMO multidisciplinary analysis and optimization conference, Indianapolis, Sept:17–19

Ravishankar B, Sankar BV, Haftka RT (2011) Uncertainty analysis of integrated thermal protection system with rigid insulation bars. In: Proceedings of the 52nd AIAA/ASME/ASCE/AHS/ASC Structures, Structural Dynamics and Materials Conference, Denver, CO, 4–7 April, AIAA Paper No. 1767

Rozvany GI, Zhou M, Birker T (1992) Generalized shape optimization without homogenization. Structural Optimization 4(3–4):250–252

Rubinstein RY (1981) Simulation and the Monte Carlo method. Wiley, New York

Sacks J, Welch WJ, Mitchell TJ, Wynn HP (1989) Design and analysis of computer experiments. Stat Sci 4(4):409–423

SAE International (2011) Formula SAE rules. http://www.studymode.com/essays/Fsae-Rules-2011-624763.html

SAE International (2016a) SAE Collegiate Design Series http://students.sae.org/cds/

SAE international (2016b) Formula SAE Events History http://students.sae.org/cds/formulaseries/history/

SAE International (2016c) About Formula SAE® Series http://students.sae.org/cds/formulaseries/about/

SAE International (2016d), Formula SAE rules http://students.sae.org/cds/formulaseries/rules

Sobol IM (2001) Global sensitivity indices for nonlinear mathematical models and their Monte Carlo estimates. Math Comput Simul 55(1):271–280

Song X, Jung J, Son H, Park J, Lee K, Park Y (2010) Metamodel-based optimization of a control arm considering strength and durability performance. Computers & Mathematics with Applications 60(4):976–980

Song X, Sun G, Li G, Gao W, Li Q (2013) Crashworthiness optimization of foam-filled tapered thin-walled structure using multiple surrogate models. Struct Multidiscip Optim 47(2):221–231

Suzuki Y, Haftka RT (2014) Analytical benchmark example for risk allocation in structural optimization. Struct Multidiscip Optim 50(1):1–7

Venter G, Scotti SJ (2012) Accounting for proof test data in a reliability-based design optimization framework. AIAA J 50(10):2159–2167

Villanueva D, Sharma A, Haftka RT, Sankar BV (2009). Risk allocation by optimization of an integrated thermal protection system. In: 8th World Congress for Structural and Multidisciplinary Optimization, Lisbon, Portugal, June

Wang G, Shan S (2007) Review of metamodeling techniques in support of engineering design optimization. ASME Trans J, Mech Des 129(4):370–380